Conformational Domains and Structural Transitions of Human von Willebrand Protein†

Joseph Loscalzo‡ and Robert I. Handin*

ABSTRACT: The conformational states of human von Willebrand protein (vWF) were studied by using ultraviolet (UV) difference, circular dichroism, and fluorescence spectrophotometric techniques in order to gain insight into the forces that maintain its asymmetric, flexible shape. vWF has 24% α-helix and 18% β-pleated sheet structure in the native state. Disulfide bond reduction and carboxamidation reduced the β-pleated sheet content by 50% without affecting the content of α-helix. In addition, the quantum yield of intrinsic (tryptophan/tyrosine) fluorescence decreased by 33% after reduction and alkylation, and the affinity of the hydrophobic fluorescent probes 8-anilino-1-naphthalenesulfonate and 6-(*p*-toluidino)-2-naphthalenesulfonate for vWF was reduced 2.5-fold. In contrast, intrinsic fluorescence quenching by acrylamide and the UV difference spectrum did not change following reduction. An analysis of changes in the intrinsic fluorescence polarization and the emission maximum shift induced by thermal and guanidine hydrochloride denaturation revealed single, smooth transitions for both native and reduced vWF, suggesting the existence of an ordered structure in both species. This study shows that (1) disulfide reduction and carboxamidation cause significant conformational changes in vWF, (2) vWF may contain discrete, ordered, conformational domains linked by regions of random polypeptide chain, and (3) specific tertiary structural domains within vWF are not affected by disulfide reduction and carboxamidation. This structural model would explain both the asymmetry and flexibility of the molecule.

The von Willebrand factor (vWF)[1] is a polymeric plasma glycoprotein comprised of a series of multimers with estimated molecular weights from 1×10^6 to 20×10^6 (Hoyer, 1981; VanDieijen et al., 1981). The basic monomer of vWF is 230000 daltons and is thought to be incorporated in the quaternary structure of the polymer through a series of covalent disulfide bonds (Counts et al., 1978; Austen et al., 1975; Peake & Bloom, 1976; Brown et al., 1976; Fukui et al., 1977; Blomback et al., 1978; Cooper et al., 1980; Gralnick et al., 1981; Martin et al., 1981). Ohmori and colleagues (Ohmori et al., 1982) have recently analyzed the morphologic features of vWF multimers by electron microscopy. They concluded that vWF polymers are flexible, thin cylinders of uniform diameter (2–3 nm) which range from 50 to 1150 nm in length (mean length 478 nm). It may be argued that the asymmetry and flexibility of vWF are important for its biological function. vWF has been shown to bind to platelets and to elements of connective tissue, which facilitates the adhesion of platelets to vascular subendothelium under conditions of high shear stress (Sakarriasen et al., 1979; Weiss et al., 1978). This function could be most effectively mediated by a glycoprotein with a large surface to volume ratio and sufficient flexibility to accommodate local hydrodynamic turbulence and vessel wall inhomogeneity.

Most previous studies of vWF have focused on the biological properties of the protein. Guided by the recent electron microscopic data (Ohmori et al., 1982), we are now in a position to characterize those physicochemical properties which influence the shape of vWF. Using a combination of spectroscopic techniques, we present a detailed analysis of the determinants of the conformation and, in turn, biological activity of vWF.

Materials and Methods

Materials. 2-ME, PEG, iodoacetamide, ANS, and tryptophan were purchased from Sigma Chemical Co., St. Louis, MO. Sodium dodecyl sulfate and acrylamide were obtained from Bio-Rad Laboratories, Richmond, CA. Ristocetin was purchased from Bio-Data Corp., Horsham, PA. TNS was obtained from Molecular Probes, Inc., Junction City, OR. Sephacryl S-1000 was obtained from Pharmacia Fine Chemicals, Uppsala, Sweden. All other materials were reagent grade or better. Deionized water was used throughout.

vWF Preparation. Unless otherwise indicated, all steps were performed in polyethylene containers at 25 °C. Two and one-half liters of plasma was obtained within 2 or 3 days of collection from the American Red Cross Blood Services, Northeast Region (Boston, MA), and frozen at −30 °C for 24 h. The resulting cryoprecipitate was thawed at 4° for 24 h and then collected by centrifugation at 5000*g* for 20 min. The pellet was resuspended in 20 mM sodium citrate and the pH adjusted to 6.1 with dropwise addition of 20 mM citric acid. Forty percent PEG (w/v) ($\langle M_r \rangle$ = 8000) was added to give a final concentration of 5%, and the resulting precipitate was discarded. Additional PEG was added to 12% and the pellet collected by centrifugation at 5000*g* for 20 min. The pellet was gently rinsed once with 10 mL of 50 mM Tris, pH 7.8, 0.15 M NaCl, 0.02% NaN_3, and 8% ethanol and once with 10 mL of 50 mM Tris, pH 7.8, 0.15 M NaCl, and 0.02% NaN_3 (column buffer). The pellet was warmed to 37 °C,

† From the Cardiology (J.L.) and Hematology (R.I.H.) Divisions, Brigham and Women's Hospital, and the Department of Medicine, Harvard Medical School, Boston, Massachusetts 02115. *Received August 9, 1983; revised manuscript received February 15, 1984.* This work was supported by Grants HL17513 and 5T32 HL07049 from the National Institutes of Health. R.I.H. is a recipient of NIH Grant RCDA HL00236.

‡ Present address: Department of Medicine, Brigham and Women's Hospital, Boston, MA 02115.

[1] Abbreviations: TBS, 10 mM Tris, pH 7.8, and 0.15 M NaCl; vWF, von Willebrand protein; vWF_r, reduced and carboxamidated vWF; ANS, 8-anilino-1-naphthalenesulfonate; TNS, 6-(*p*-toluidino)-2-naphthalenesulfonate; Gdn·HCl, guanidine hydrochloride; CD, circular dichroism; 2-ME, 2-mercaptoethanol; PEG, poly(ethylene glycol); Tris, tris(hydroxymethyl)aminomethane; UV, ultraviolet; SDS, sodium dodecyl sulfate; DTNB, 5,5′-dithiobis(2-nitrobenzoic acid); PAGE, polyacrylamide gel electrophoresis.

0006-2960/84/0423-3880$01.50/0

dissolved in approximately 10 mL of column buffer, and applied to a siliconized glass column containing Sephacryl S-1000 (95 × 2.5 cm). Four-milliliter fractions were collected at a flow rate of 70 mL/h.

Fractions were analyzed for protein concentration and for ability to support ristocetin-dependent platelet agglutination. Fractions were stored at 4 °C for up to 5 days or at −30 °C in 50% glycerol for up to 5 weeks without an appreciable loss of vWF activity. Unless otherwise indicated, the most active fractions, which typically had ristocetin activities of 400 units/mg of protein, were used in all studies. Protein purity was monitored by SDS–polyacrylamide gel electrophoresis after reduction with 2-ME (50 mM) in the presence of 2% SDS. Gel electrophoresis was carried out by the technique of Weber & Osborne (1969), as modified by Laemmli (1970). After denaturation and reduction, most active column fractions typically demonstrated a single 230 000-dalton band (Legaz et al., 1973). Average protein yields were 3 mg/2.5 L of plasma. vWF was concentrated, when necessary, by ultracentrifugation at 100000*g* for 2 h at 4 °C or by dialysis against 40% (w/v) PEG ($\langle M_r \rangle$ = 20 000) at 4 °C. Protein concentrations were estimated by the method of Lowry (1951).

vWF Activity. The ability of vWF to agglutinate formalin-fixed platelets (Allain et al., 1975) was determined by using the ristocetin assay (Howard & Firkin, 1976; Olson et al., 1975). To 0.2 mL of formalinized platelets at $4 \times 10^5/\mu L$ in TBS was added 0.25 mL vWF at the desired final concentration. The mixture was incubated at 37 °C with stirring at 900 rpm in a Payton dual-channel aggregometer (Payton Associates, Inc., Buffalo, NY) and the agglutination reaction initiated by addition of 0.05 mL of 10 mg/mL ristocetin. Changes in the light transmittance of the mixture were recorded by using an Omniscribe recorder (Houston Instruments, Austin, TX). In all cases, activity curves were constructed as plots of maximal velocity of aggregation vs. log vWF concentration and compared with reference plasma standards assayed by serial dilution. These plots were linear over a range of final vWF concentrations of 0.5–50 μg/mL. One unit of activity was arbitrarily defined as that contained in an equal volume of normal plasma.

Disulfide Reduction and Alkylation. vWF was treated with 50 mM 2-ME in 50 mM Tris-HCl, pH 7.4, for 1 h at 25 °C without any denaturing reagents followed by 60 mM iodoacetamide in the same buffer to produce vWF_r. Extensive dialysis against TBS was then performed to remove unbound reactants. This degree of reduction repeatedly exposed approximately 125 of the 151 total (Legaz et al., 1973) sulfhydryl groups per mole of monomer (*all* of which are disulfide-linked in the native protein) as assayed by using the 5,5′-dithiobis-(2-nitrobenzoic acid) (DTNB) method (Ellman, 1959; Habeeb, 1966). After addition of 2-ME to a final concentration of 50 mM, 0.4 mL of 0.1 mg/mL vWF was removed from the incubation solution and the protein precipitated with 25% ice-cold trichloroacetic acid (v/v). The sample was centrifuged at 25 °C in a Beckman microfuge (Beckman Instruments, Inc., Fullerton, CA) at 8700*g* for 4 min. The pellet was washed 3 times with 25% ice-cold trichloroacetic acid and redissolved in 1 mL of 10 mM Tris, pH 7.8, 0.15 M NaCl, 8 M urea, and 5% SDS. To 0.8 mL of this solution was added 0.2 mL of 0.5 mg/mL DTNB. After 20 min, the absorbance at 410 nm was measured and adjusted by subtracting the absorbance of reagent and protein blanks. A molar extinction coefficient of 14 200 M^{-1} cm^{-1} for the nitrothiophenolate ion was used to calculate the concentration of free sulfhydryl groups (Collier, 1973). Repeated assays at 2 and 5 h after reduction failed to demonstrate a significant change in free sulfhydryls exposed. That alkylation was complete under these conditions was demonstrated by precipitating vWF_r and showing that DTNB failed to react with the modified protein.

Reduction and alkylation, as performed in these experiments, completely eliminated ristocetin-dependent platelet-agglutinating activity. SDS–PAGE analysis of vWF after reduction and alkylation revealed a single band wiith a mobility on 5% polyacrylamide gels identical with that of the fibronectin dimer. Upon further reduction in the presence of 2% SDS, this converted to a band with a mobility identical with that of fibronectin monomer. This partially reduced species of vWF, with an apparent $\langle M_r \rangle$ of 440 000, was used in all the spectroscopic studies described below. The loss of activity occurs because platelet agglutination depends critically on vWF polymer size (Martin et al., 1981; Ohmori et al., 1982), smaller polymers having lesser activity.

UV Spectrophotometry. Absorption measurements were performed in a Gilford Model 2400 spectrophotometer (Gilford Instrument Laboratories, Inc., Oberlin, OH). Spectra were recorded by using split-compartment cells containing 0.8 mL each of protein and buffer solutions. Difference spectra were obtained by subtracting spectra taken at pH 7.8 from those recorded at pH 11.5.

Fluorescence Spectrophotometry. Fluorescence measurements were performed on a Perkin-Elmer Model 44B spectrofluorometer (Perkin-Elmer Corp., Norwalk, CT) equipped with a thermostated cell holder and Hitachi polarizers. The absorbance of solutions was less than 0.1 at exciting wavelengths. A reference cell containing rhodamine B was used to correct for variation and nonlinearity in the excitation source.

Quantum yields were obtained by excitation at 280 or 295 nm, using the method of Parker & Rees (1960):

$$A_p/A_r = Q_pD_p/(Q_rD_r) \quad (1)$$

where A is the area under the fluorescence spectrum and D is the optical density at the exciting wavelength. The subscripts p and r refer to protein and reference solution, respectively. A value of 0.20 for Q_{Trp} was used (Teale & Weber, 1957; Kronman & Holmes, 1971).

Since tyrosine quantum yields cannot be measured directly from the recorded spectra, they were calculated from the protein and tryptophan quantum yields (Kronman & Holmes, 1971) by using the following equation:

$$Q_{Tyr} = Q'_{Tyr}/[1 + (m/n)(\epsilon_{Trp}/\epsilon_{Tyr})] \quad (2)$$

where m and n are the number oftryptophan and tyrosine residues per protein molecule, respectively, $\epsilon_{Trp}/\epsilon_{Tyr}$ is the ratio of free amino acid extinction coefficients, Q'_{Tyr} is estimated from

$$Q'_{Trp} = Q_{Pro} - Q'_{Trp} \quad (3)$$

and Q'_{Trp} is derived from the amplitude (F) and area (A) of the emission spectra as

$$Q_{Trp} = Q'_{Trp}[(F/A)_{\lambda=280}/(F/A)_{\lambda=295}] \quad (4)$$

The polarization of fluorescence emission was calculated from

$$P = (I_{VV} - GI_{VH})/(I_{VV} + GI_{VH}) \quad (5)$$

where $G = I_{HV}/I_{HH}$, I is the fluorescence intensity, and the first and second subscripts refer to the plane of polarization of the excitation and emission beams, respectively (V, vertical; H, horizontal).

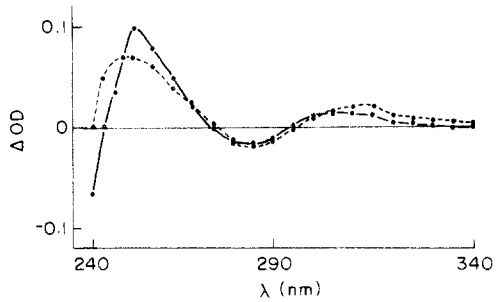

FIGURE 1: Difference absorption spectra of vWF in the near-UV region. Spectra were obtained for vWF (—) and vWF_r (---) by subtracting spectra at pH 7.8 from those at pH 11.5 at 25 °C in 1-cm path-length cells.

Table I: Protein, Tryptophan, and Tyrosine Quantum Yields of Human von Willebrand Protein[a]

	Q_p (λ_{max})[d]	Q_{Trp} (λ_{max})[e]	Q_{Tyr}
vWF[b]	0.166 (324)	0.173 (330)	0.011
vWR_r[b]	0.112 (327)	0.143 (331)	0.004
denatured vWF[c]	0.098 (311s, 332)	0.110 (336)	0.003
denatured vWF_r[c]	0.065 (313s, 347)	0.088 (347)	0.001

[a] The values of the quantum yields and emission maxima are averages obtained from two measurements, with deviations of ±5% and ±1 nm, respectively. [b] In TBS. [c] In 6 M Gdn·HCl–TBS. [d] Excitation at 280 nm. [e] Excitation at 295 nm.

Fluorescence intensities were corrected for the self-absorption of incident light in the ANS and TNS titration by using the relationship

$$I_{cor} = I_{obsd}[2.303\epsilon_{\lambda_{max}}F/(1 - 10^{-\epsilon_{\lambda max}F})] \quad (6)$$

where F refers to the total dye concentration, ϵ is the molar absorptivity of the dye ($\epsilon_{363,ANS} = 4.91 \times 10^3$ M^{-1} cm^{-1}, $\epsilon_{358,TNS} = 5.43 \times 10^3$ M^{-1} cm^{-1}), and I_{cor} and I_{obsd} refer to the corrected and observed intensities, respectively (McClure & Edelman, 1966).

CD Spectrophotometry. CD spectra were recorded by using a Carey Model 15 spectropolarimeter (Varian Instruments, Sunnyvale, CA) with a CD accessory and equipped with a temperature-controlled cell holder. Quartz cells of 0.5-cm path length were used. Two or three measurements were made for each sample, and excellent reproducibility was obtained at 2.5 nm/min with a pen period of 3 s. The spectra were corrected for the base line obtained with buffer solvent. Molar ellipticity values per residue were obtained by using 112 as the mean residue weight (Legaz et al., 1973) with the values expressed as degrees centimeter squared per decimole. The data were fitted by a computer program based on the method of Chen and colleagues (Chen et al., 1974) using an average segment of 10 residues.

Results

Secondary and Tertiary Structure. (A) UV Absorption. The absorption difference spectra in the far-UV region for vWF and vWF_r are shown in Figure 1. These spectra are similar, with two positive bands at 250 and 290–305 nm and a negative band at 280 nm. The positive band at the longer wavelength is likely due to vibronic structure.

(B) Fluorescence. The quantum yield and emission maxima for vWF and vWF_r and their denatured forms are shown in Table I. The quantum yields obtained by exciting at 280 nm are protein quantum yields and are due to tryptophan and tyrosine fluorescence. The quantum yields obtained by exciting at 295 nm result primarily from tryptophan emission. The tyrosine quantum yields calculated by subtracting tryptophan from protein quantum yields are also listed in Table I. They

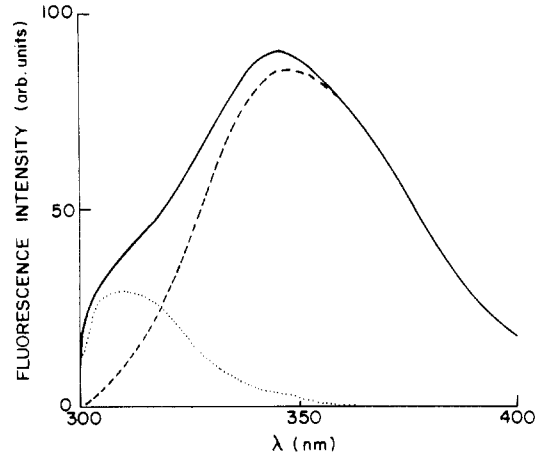

FIGURE 2: Resolution of tyrosine fluorescence from tryptophan fluorescence in denatured vWF. Emission spectra of 0.09 mg/mL vWF in TBS, pH 7.8, at 25 °C were recorded by exciting at 280 nm (—) and 295 nm (---) with normalization above 360 nm. The difference between the two spectra (···) represents tyrosine fluorescence.

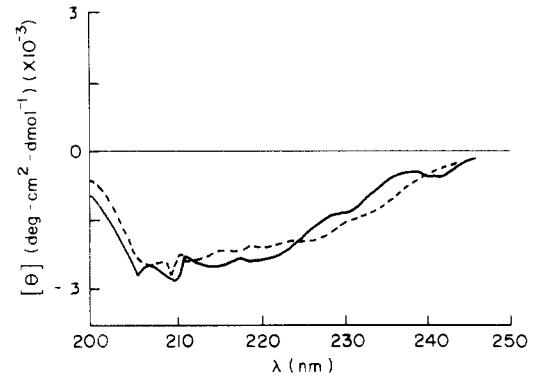

FIGURE 3: Far-UV circular dichroism (CD) spectra of vWF. Spectra were recorded at 0.25 mg/mL vWF (—) and vWF_r (---) in TBS, pH 7.8, at 25 °C. The spectra were invariant over time during multiple scans at 2.5 nm/min with an instrument time constant of 3 s.

were calculated from eq 4 by using a ratio of tryptophan to tyrosine in vWF determined from the amino acid composition (Legaz et al., 1973) and a value of 4 for the ratio $\epsilon_{Trp}/\epsilon_{Tyr}$ (Weber & Young, 1964). The three quantum yields obtained for each vWF species are comparable with those of many other proteins (Kronman & Holmes, 1971). After reduction and alkylation, the protein quantum yield of vWF decreased by 33%, while the tryptophan quantum yield decreased by 17%. Denaturation reduced the protein quantum yield by 40% for vWF and by 42% for vWF_r and the tryptophan quantum yield by 36% for vWF and by 38% for vWF_r. The tyrosine quantum yield is very small in all cases and much lower than that recorded for the free amino acid, 0.21 (Teale & Weber, 1957).

The emission maxima of vWF and vWF_r when excited at 280 nm are shifted to wavelengths shorter than that of free tryptophan. vWF shows a larger blue shift of the emission maximum (324 nm) than does vWF_r (327 nm) (Table I). In the presence of 6 M Gdn·HCl, the emission maxima of both species shift to longer wavelengths (332 nm for vWF and 347 nm for vWF_r). When excited at a shorter wavelength (270 nm), a shoulder at 311 and 313 nm was observed for vWF and vWF_r, respectively. This tyrosine emission band was not visible with excitation at 280 nm unless the protein was denatured with Gdn·HCl. By exciting first at 280 nm, where both tyrosine and tryptophan are excited, and then at 295 nm, where predominantly tryptophan is excited, and normalizing one emission spectrum to the other above 360 nm, we obtained a

Table II: Ordered Secondary Structure of von Willebrand Protein by UV CD Spectroscopy

	α-helix (%)	β-pleated sheet (%)	random coil (%)
vWF	24	18	58
vWF_r	24	8	68

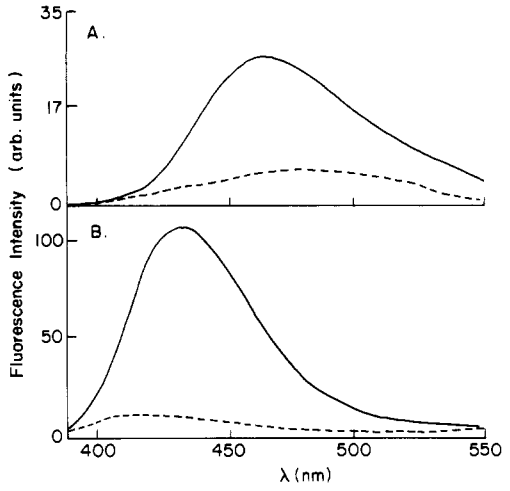

FIGURE 4: Effect of vWF on fluorescence emission of ANS and TNS. Spectra were recorded in the ratio mode in TBS, pH 7.8, with 5-nm excitation and emission bandwidths. (A) 120 μM ANS in TBS (---) and in TBS containing 0.09 mg/mL vWF (—), excitation at 350 nm. (b) 53 μM TNS in TBS (---) and in TBS containing 0.08 mg/mL vWF (—), excitation at 350 nm.

difference spectrum representing the contribution of tyrosine to the intrinsic vWF fluorescence (Figure 2).

(*C*) *Circular Dichroism.* The CD spectra of vWF and vWF_r in the far-UV region afford information about the secondary structure of the protein. Figure 3 shows that both species have some ordered secondary structure. The data were fitted by a computer program based on the method of Chen and colleagues (Chen et al., 1974) over the wavelength range of 201–250 nm. The percentages of α-helix, β-pleated sheet, and random coil calculated for each species are shown in Table II. Given the limitations of the computer fit, it appears that a significant amount of ordered secondary structure exists in vWF and that sulfhydryl reduction and carboxamidation of vWF halve the content of β-pleated sheet structure without changing the amount of α-helix.

(*D*) *ANS and TNS Binding.* The fluorescence emission spectra of ANS and TNS in the presence and absence of vWF are shown in Figure 4. The fluorescence of both probes was strongly enhanced in the presence of vWF. On a molar basis, TNS bound to vWF was more intensely fluorescent than ANS bound to vWF.

Fluorescence titration of 413 nM vWF and vWF_r with ANS and TNS was used to estimate the affinity constants for the binding of these fluorophores to the protein. Using low vWF concentrations such that $[ANS]_{bound} \ll [ANS]_{total}$ and $[TNS]_{bound} \ll [tNS]_{total}$ at all concentrations of ANS and TNS permits the latter concentration in each case to be used as a fair approximation of the free ligand concentration. Under these conditions, Scatchard plots can be constructed by using corrected fluorescence enhancement to follow bound ligand (Scatchard, 1949; Wang & Edelman, 1971; Glademans & Jolley, 1980). Such plots are depicted in Figure 5. These data show that vWF had about 2.5-fold greater affinity than vWF_r for both fluorophores.

(*E*) *Acrylamide Quenching.* Figure 6 shows the effect of the fluorescence quencher, acrylamide, on the intrinsic

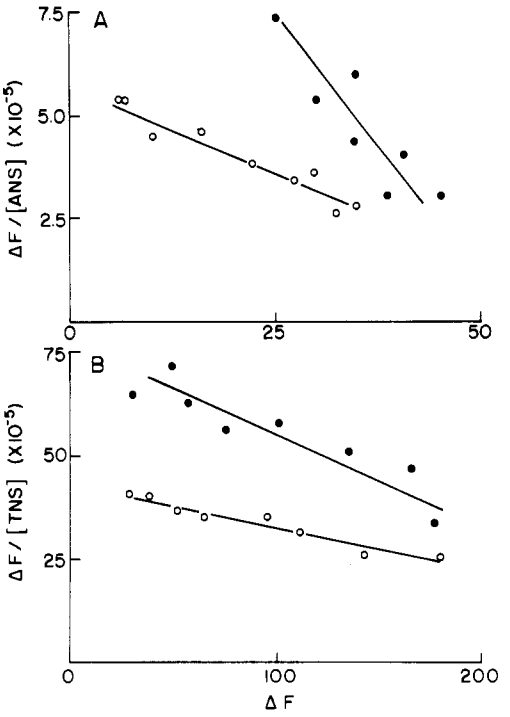

FIGURE 5: Fluorescence enhancement titrations of ANS and TNS binding to vWF. Titrations were performed by addition of small volumes of 2.3 mM ANS or 0.46 mM TNS in TBS to a 1.5-mL sample of vWF of vWF_r in TBS, pH 7.8, at 25 °C. Parallel titrations were done with 1.5 mL of TBS to allow correction for the fluorescence of free ligand. Following substraction of buffer blanks, the net fluorescence was corrected for dilution and inner filter effects as described under Materials and Methods. Binding data are presented as Scatchard plots according to Glaudemans & Jolley (1980). (A) ANS titration of 0.09 mg/mL vWF (●) and vWF_r (○) using ANS concentrations of 11–120 μM (excitation at 350 nm and emission at 469 nm). Estimated K_{diss} values were found to be 40 μM for vWF and 110 μM for vWF_r. (B) TNS titration of 0.09 mg/mL vWF (●) and vWF_r (○) using TNS concentrations of 2–70 μM (excitation at 350 nm and emission at 435 nm). Estimated K_{diss} values were found to be 40 μM for vWF and 90 μM for vWF_r.

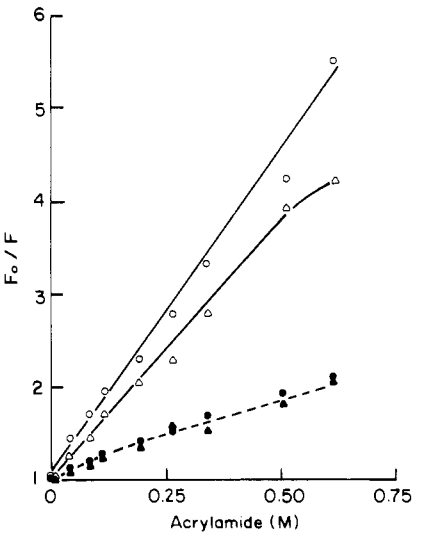

FIGURE 6: Steady-state intrinsic fluorescence intensity quenching of vWF by acrylamide. Fluorescence intensity was recorded in TBS, pH 7.8, at 25 °C for vWF (circles) and vWF_r (triangles) in the absence (closed symbols) and presence (open symbols) of 6M Gdn·HCl. Titrations were performed by addition of small volumes of 5 M acrylamide in TBS, pH 7.8, to a 1.5-mL sample of protein at 0.034 mg/mL (excitation at 280 nm and emission at 340 nm). F_0 represeants the fluorescence intensity in the absence of acrylamide, and F represents the fluorescence intensity at a given concentration of acrylamide.

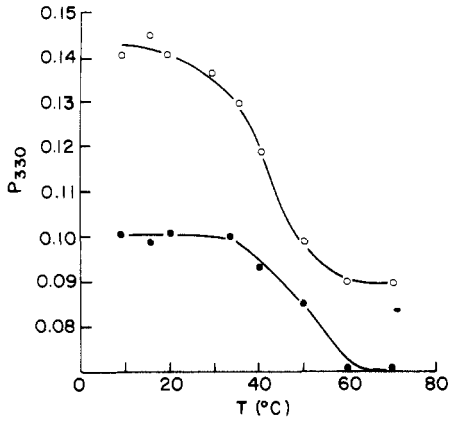

FIGURE 7: Effect of temperature on the intrinsic fluorescence polarization of vWF. Intrinsic fluorescence polarization was recorded for vWF (●) and vWF_r (○) each at 0.08 mg/mL in TBS, pH 7.8 (excitation at 280 nm and emission at 330 nm).

fluorescence intensity of vWF and vWF_r. The Stern–Volmer plots suggest that both static and dynamic (collisional) processes contribute to the quenching of fluorescence intensity of the intrinsic protein fluorophores. No upward curvature is noted, implying that the static quenching parameter is small. Downward curvature is present in all cases, suggesting the presence of multiple emission components (Lehrer & Leavis, 1978). Denaturation of vWF and vWF_r leads to a marked enhancement of the slope of the Stern–Volmer plots, suggesting that the denaturation process alters sufficient amounts of ordered structure to permit greater quencher access to the immediate environment of the intrinsic fluorophores.

Structural Transitions. The apparent flexibility of vWF and its marked asymmetry and uniform width suggest that its shape on electron micrographs may be the result of an ordered structure composed of discrete domains connected by random polypeptide segments which comprise the backbone of the molecule. In order to determine whether ordered domains are present, the effects of temperature and Gdn·HCl on vWF were evaluated since noncovalent interactions between side chains in proteins are eliminated by these two denaturing conditions. Tertiary structural changes were evaluated from the fluorescence of tyrosine and tryptophan residues. These two side chains can be used as conformational probes since they are two of the most hydrophobic groups present in proteins and are generally sequestered within the matrix of most proteins (Stryer, 1968; Edelhoch & Osborne, 1976).

(*A*) *Temperature.* The temperature dependence of fluorescence polarization has been used to measure the relaxation times of proteins by application of the Perrin equation (Chen et al., 1969). The relaxation time for vWF could not be measured by this procedure since the fluorescence lifetime of tryptophan is too short relative to the rotational correlation time for vWF. No change in fluorescence polarization was observed for vWF and vWF_r until about 30° for vWF and 20° for vWF_r at pH 7.8 (Figure 7). Moreover, 90% ethylene glycol had no effect on polarization, suggesting that the intrinsic polarization is very near its limiting value (i.e., that observed in the absence of rotational events within the lifetime of the excited state) and, therefore, precludes a random polypeptide structure for vWF or vWF_r. The limiting value of tryptophanyl polarization observed in several low molecular weight polypeptide hormones with little or no organized structure (adrenocorticotropic hormone, calcitonin, glucagon) is much lower, i.e., near 0.04 at 25 °C (Alexander et al., 1979). Since the fluorescence polarization was greater for vWF_r than for vWF, there is likely to be some additional rotational

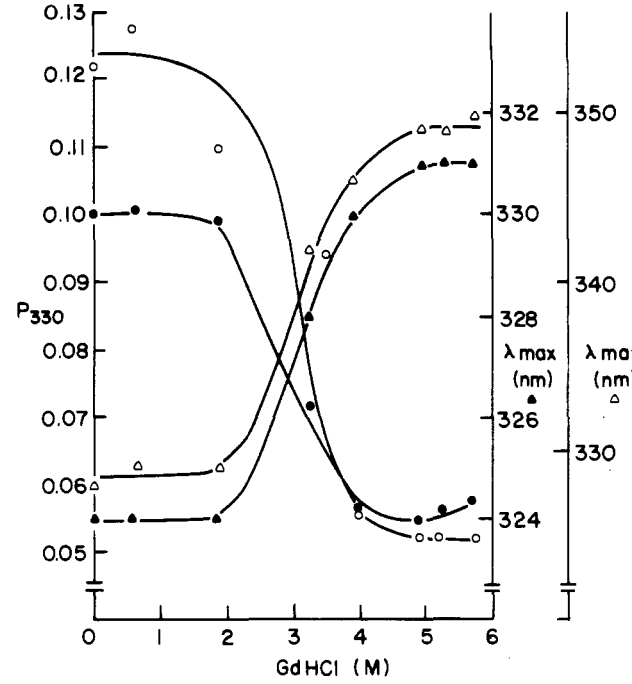

FIGURE 8: Effect of Gdn·HCl concentration on the intrinsic fluorescence polarization and emission maximum of vWF. Fluorescence measurements were recorded for vWF (closed symbols) and vWF_r (open symbols) each at 0.08 mg/mL in TBS, pH 7.8, at 25 °C. The emission maximum (triangles) and the fluorescence polarization (circles) (excitation at 280 nm, emission at 330 nm) were recorded as a function of Gdn·HCl concentration.

freedom for the bulk of intrinsic fluorophores in the native state which is significantly hindered after reduction and carboxamidation of vWF.

The fluorescence polarization was used to follow the transition of vWF and vWF_r to less ordered conformational states. The fluorescence polarization of both vWF and vWF_r falls precipitously between 30 and 60 °C. While the polypeptide structures of both species become more disordered with heating, the temperature range over which the transition occurred in vWF_4 was somewhat broader than that in vWF, suggesting a greater thermal stability of the disulfide-linked polymer than the reduced and carboxyamidated species.

(*B*) *Gdn·HCl Concentration.* The effect of Gdn·HCl concentration on two fluorescent parameters, intrinsic polarization and emission maximum, for vWF and vWF_r is shown in Figure 8. Only a single transition is noted by both measurements with the midpoints of the curves near 3 M Gdn·HCl. In each case, the limiting values of the fluorescent parameters are those expected for a highly disordered polypeptide chain. Both vWF and vWF_r underwent similar transitions in polarization and emission maxima; however, the absolute value for these changes was significantly different between the two species. When the polarization of vWF in Gdn·HCl was measured after 24 h, no further change was observed.

Discussion

This study was undertaken to elucidate which features of the secondary and tertiary structure of vWF determine its shape in solution and thereby influence molecular function. This is a particularly difficult task because of the size and heterogeneity of vWF oligomers. In addition, as in all spectroscopic studies, the interpretations are also limited by the fact that one usually records average signals from multiple regions of a given molecule. Despite these limitations, we were able to obtain spectroscopic data which provide new insights into the secondary and tertiary structure of vWF polymers.

There are several features of the vWF molecule which were exploited in our experimental approach to simplify the analysis and interpretation of the data presented here. It has been reasonably well established that all species of vWF are oligomers of a single polypeptide subunit. The ability to depolymerize vWF by disulfide bond reduction permits us to test which conformational features are unique to the polymer and which are retained by its smaller subunits. Moreover, because of these properties, it is likely that the secondary and tertiary structural features we have identified are not unique to one region of the polymer but are repeated along the polymer chain and that conformational features are uniform and repeat along the length of the polymer. It is also of interest that some of the parameters we measured did not change after reduction and alkylation, despite the fact that we observed a dissociation of the vWF polymer into smaller subunits. This suggests that disulfide reduction depolymerizes vWF without perturbing many of the secondary and tertiary structural features of the protomeric units which assemble to produce the polymer. For example, UV difference absorption spectra for vWF and vWF_r were very nearly identical. Because the absorption differences induced by alkaline denaturation are similar, the microenvironments of the subclass of intrinsic chromophores perturbed by alkalinity must also be similar.

Analysis of intrinsic protein fluorescence, however, reveals different information about the bulk of fluorophores in vWF. The intrinsic fluorescence of vWF is predominantly due to tryptophan. Despite the presence of approximately 46 tyrosine residues per 230 000-dalton vWF monomer, the fluorescence of the estimated 57 tryptophan residues per 230 000-dalton monomer (Legaz et al., 1973) dominates protein fluorescence. For many proteins, it has been possible to obtain a shoulder for the tyrosine emission at 305–310 nm when excited at 275–280 nm (Andley & Chakrabarti, 1982). For vWF, no such shoulder is observed unless the protein is denatured. This may indicate that the energy transfer from tyrosine to tryptophan is more efficient in native vWF than in many other proteins. On denaturation, this efficiency of energy transfer is obviously decreased, making the tyrosine emission quite visible. Another potential explanation for the absence of the tyrosine shoulder is that a screening effect, rather than energy transfer, is responsible for the disappearance of the tyrosine emission in most tryptophan-containing protein fluorescence spectra in nondenatured states (Konev, 1967). Nonetheless, a Förster resonance transfer mechanism between tyrosine and tryptophan fits well with the experimental results of many proteins (Kronman & Holmes, 1971).

The wavelength of the emission maximum of vWF indicates that most of the tryptophan residues are buried in the hydrophobic matrix of the protein. Disulfide reduction and carboxamidation tend to shift the emission maximum to longer wavelengths and decrease the quantum yield. Although neither the emission maximum nor the quantum yield can be a simple function of the degree of exposure of tryptophan residues (Kronman & Holmes, 1971; Weinrbb & Steiner, 1970), the combination of a red shift of the emission maximum and a decrease in the quantum yield argues that tryptophan residues buried in vWF are exposed following reduction and alkylation.

The two hydrophobic probes, ANS and TNS, have also been found to bind to vWF and vWF_r with alteration in their fluorescence spectra. A decrease in solvent polarity and, to some extent, an increase in rigidity of the local environment have been demonstrated to increase the quantum yield and decrease the wavelength of fluorescence emission of arylaminonaphthalenesulfonates (McClure & Edelman, 1966; Stryer, 1965; Turner & Brand, 1968). By comparison of the shift in the emission maximum measured in solvents of decreasing polarity, the polarity of the binding site(s) for ANS and TNS on vWF may be determined by using the empirical solvent polarity value, Z, of Kosower (1958). The shift in fluorescence maxima of ANS and TNS in the presence of vWF and vWF_r compared with that in water suggests that Z_{est} for ANS and TNS binding to vWF and vWF_r is approximately 80 (Turner & Brand, 1968), a value consistent with that found in other proteins with specific, relatively apolar hydrophobic binding sites. The high affinity of binding for both species for vWF and vWF_r and the linearity of the Scatchard plots argue that a single, high-affinity site (or several sites of equally high affinity) for small hydrophobic probes exists on vWF. Reduction and carboxamidation of vWF reduced the affinity of vWF for these probes 2.5-fold. This is a small but significant change and suggests that this hydrophobic binding domain is affected by reduction.

Acrylamide quenches the intrinsic fluorescence of vWF and vWF_r similarly. While one might expect differences in quenching between these two species based on the differences in intrinsic quantum yields and in ANS and TNS binding, the observed similarity may simply reflect the averaged effects of quenching many fluorophores in different microenvironments. In support of this hypothesis, the downward curvature of the Stern–Volmer plots implies the existence of multiple emission components. In contrast, the difference in slope of the Stern–Volmer plot between denatured vWF and vWF_r may reflect differences in exposure of denatured, fluorophore-containing regions of protein to solvent; denatured vWF, being constrained by the intermonomeric disulfide linkages, may be unable to "bury" the intrinsic fluorophores within random hydrophobic domains as well as denatured vWF_r. That the intrinsic fluorescence emission maximum for denatured vWF is less than that for denatured vWF_r shows that the bulk of fluorophores in denatured vWF is still in more hydrophobic domains than in vWF_r, while the slightly increased quenching by acrylamide of the fluorescence of denatured vWF compared with denatured vWF_r shows that these hydrophobic microenvironments have greater solvent access in denatured vWF than in denatured vWF_r.

In contrast to the changes in tertiary structure implied by the shifts in tryptophan fluorescence and binding of ANS and TNS, the CD spectra demonstrate that considerable ordered secondary structure remains after disulfide reduction and carboxamidation of vWF. In fact, the content of α-helix does not change at all. On the other hand, β-pleated sheet structure is reduced by 50% when compared to native vWF. Ohmori and colleagues (Ohmori et al., 1982) have noted that with progressive disulfide reduction, the linear, extended, asymmetric vWF molecule essentially "balls up" into a more compact, spherical form. It is tempting to speculate that some of the extended segmental domains of vWF are in the β-pleated sheet conformation, which, after disulfide reduction and carboxamidation, is destabilized and forced into a more energetically favorable random-coil conformation. This may result in the more compact structure noted on electron micrographs.

The thermal and Gdn·HCl denaturation curves suggest that ordered regions persist in vWF_r despite the gross morpholigical changes noted after reduction and carboxamidation. For both vWF and vWF_r, the transition curves resemble those seen with many globular proteins of low molecular weight (Privalow & Khechinashvili, 1974). The thermal and Gdn·HCl transition curves, as measured by fluorescence polarization and emission

maxima, reveal only a single, broad transition for both species. These broad melting curves may represent several independent transitions with slightly different values of transition midpoints.

The best way to reconcile the flexibility of vWF with the observed denaturation curves (which are usually seen in more ordered, globular proteins) and with the accompanying loss of β-pleated sheet content in vWF_r is to consider vWF as composed of several discrete domains of β-pleated sheet structure, possessing some rotational freedom with respect to one another and interconnected by randomly organized polypeptide segments. These interconnecting random polypeptide segments may contain some of the many prolines (8%) found by amino acid analysis of vWF (Legaz et al., 1973). The structure of fibrinogen is similar organized (Hall & Slayter, 1959), as is that of fibronectin (Alexander et al., 1978, 1979).

In summary, this study shows the following: (1) conformational changes occur in vWF after disulfide reduction and carboxamidation and can be demonstrated by changes in the intrinsic fluorescence, quantum yield, emission maximum, and ANS and TNS binding; (2) specific tertiary structural domains of vWF are not affected by disulfide reduction and carboxamidation, as shown by the similarity in UV difference absorption and acrylamide quenching; (3) vWF contains a moderate amount of ordered secondary structure which is partly modified by disulfide reduction and carboxamidation; and (4) vWF contains discrete, ordered, conformational domains which are probably linked by regions of random polypeptide chain, possibly accounting for the asymmetry and flexibility of the molecule.

Acknowledgments

We thank Drs. Elkan Blout, H. Franklin Bunn, and Thomas Rounds for assistance with the CD spectra and for helpful discussions.

Registry No. vWF, 9001-27-8; acrylamide, 79-06-1.

References

Alexander, S. S., Jr., Colonna, G., Yamada, K. M., Pastan, I., & Edelhoch, H. (1978) *J. Biol. Chem. 253*, 5820–5824.

Alexander, S. S., Jr.; Colonna, G., & Edelhoch, H. (1979) *J. Biol. Chem. 253*, 5820–5824.

Allain, J. P., Cooper, J. A., Wagner, R. H., & Brinkaus, K. M. (1975) *J. Lab. Clin. Med. 85*, 318–328.

Andley, V. P., & Chakrabarti, B. (1982) *Photochem. Photobiol. 35*, 385–390.

Austen, D. E. G., Carey, M., & Howard, M. A. (1975) *Nature (London) 253*, 55–56.

Blomback, B., Hessel, B., Savidge, G.,Wikstrom, L., & Blomback, M. (1978) *Thromb. Res. 12*, 1177–1194.

Brown, J. E., Baugh, R., & Hougie, C. (1976) *Thromb. Res. 8*, 777–783.

Chen, R. F., Edelhoc, H., & Steiner, R. F. (1969) in *Physical Priciples and Techniques of Protein Chemistry (Part A)* (Leach, S. J., Ed.) pp 171–244, Academic Press, New York.

Chen, Y.-H., Yang, J. T., & Chau, K. H. (1974) *Biochemistry 13*, 3350–3359.

Collier, H. B. (1973) *Anal. Biochem. 56*, 310–311.

Cooper, H. A., Barnes, D. S., Lawler, F. S., Jr., & Wagner, R. H. (1980) in *Regulation of Coagulation* (Mann, K. G., & Taylor, F. B., Eds.) pp 337–344, Elsevier/North-Holland, New York.

Counts, R. B., Paskell, S. L., & Elgee, S. K. (1978) *J. Clin. Invest. 62*, 702–709.

Edelhoch, H., & Osborne, J. C. (1976) *Adv. Protein Chem. 30*, 183–250.

Ellman, G. L. (1959) *Arch. Biochem. Biophys. 82*, 70–77.

Fukui, H., Mikami, S., Okuda, T., Murashima. T., & Yoshioka, A. (1977) *Br. J. Haematol. 36*, 259–270.

Glaudemans, C. P. J., & Jolley, M. E. (1980) *Methods Carbohydr. Chem. 8*, 145–149.

Gralnick, H. R., Williams, S. B., & Morisato, D. K. (1981) *Blood 58*, 387–397.

Habeeb, A. F. S. A. (1966) *Biochim. Biophys. Acta 115*, 440–454.

Hall, C. E., & Slayter, H. S. (1959) *J. Biophys. Biochem. Cytol. 5*, 11–15.

Howard, M. A., & Firkin, B. G. (1976) *Thromb. Haemostasis 26*, 326–369.

Hoyer, L. (1981) *Blood 58*, 1–13.

Konev, S. V (1967) *Fluorescence and Phosphorescence of Proteins and Nucleic Acids*, Plenum Press, New York.

Kosower, E. M. (1958) *J. Am. Chem. Soc. 80*, 3253–3260.

Kronman, M. J., & Holmes, L. G. (1971) *Photochem. Photobiol. 14*, 113–134.

Laemmli, U. K. (1970) *Nature (London) 227*, 680–682.

Legaz, M. E., Schmer, G., Counts, R. B., & Davie, E. W. (1973) *J. Biol. Chem. 248*, 3946–3955.

Lehrer, S. S. & Leavis, P. C. (1978) *Methods Enzymol. 49*, 222–236.

Lowry, O. H., Rosebrough, N. J., Farr, A. L., & Randall, R. (1951) *J. Biol. Chem. 193*, 265–275.

Martin, S. E., Marder, V. J., Francis, C. W., & Barlow, G. H. (1981) *Blood 57*, 313–323.

McClure, W. O., & Edelman, G. N. (1966) *Biochemistry 5*, 1908–1919.

Ohmori, K., Fretto, L. J., Harrison, R. L., Switzer, M. E. P., Erickson, H. P., & McKee, P. A. (1982) *J. Cell Biol. 95*, 632–640.

Olson, J. D., Brockway, W. J., Fass, D. N., Magnusson, M. A., & Bowie, E. J. W. (1975) *Am. J. Clin. Pathol. 63*, 210–218.

Parker, C. A., & Rees, W. T. (1960) *Analyst (London) 85*, 587–600.

Peake, I. R., & Bloom, A. L. (1976) *Thromb. Haemostasis 35*, 191–201.

Privalov, P. L., & Khechinashvili, N. N. (1974) *J. Mol. Biol. 86*, 665–684.

Sakarriasen, K. S., Bolhuis, P. A., & Sixma, J. J. (1979) *Nature (London) 279*, 636–638.

Scatchard, G. (1949) *Ann. N.Y. Acad. Sci. 51*, 660–672.

Stryer, L. (1965) *J. Mol. Biol. 13*, 482–495.

Stryer, L. (1968) *Annu. Rev. Biochem. 37*, 25–50.

Teale, F. W. J., & Weber, G. (1957) *Biochem. J. 65*, 476–482.

Turner, O. C., & Brand, L. (1968) *Biochemistry 7*, 3381–3390.

VanDieijen, G., Tans, G., Rosing, J., & Hemker, H. C. (1981) *J. Biol. Chem. 256*, 3433–3442.

Wang, J. L., & Edelman, G. M. (1971) *J. Biol. Chem. 246*, 1185–1191.

Weber, G., & Young, L. B. (1964) *J. Biol. Chem. 239*, 1424–1431.

Weber, K., & Osborne, M. (1969) *J. Biol. Chem. 244*, 4406–4412.

Weinryb, I., & Steiner, R. F. (1970) *Biochemistry 9*, 135–146.

Weiss, H. J., Turitto, V. J., & Baumgartner, H. R. (1978) *J. Lab. Clin. Med. 92*, 750–764.